

The Galactic Bar

Ortwin Gerhard and Christopher Wegg

Abstract The Milky Way's bar dominates the orbits of stars and the flow of cold gas in the inner Galaxy, and is therefore of major importance for Milky Way dynamical studies in the Gaia era. Here we discuss the pronounced peanut shape of the Galactic bulge that has resulted from recent star count analysis, in particular from the VVV survey. We also discuss the question whether the Milky Way has an inner disk pseudo-bulge, and show preliminary evidence for a continuous transition in vertical scale-height from the peanut bulge-bar to the planar long bar.

1 Introduction

The Gaia satellite will soon provide us with exquisite data for the motions of stars in our Galaxy. The Milky Way's stellar bar has a strong influence on the orbits of stars inside the solar circle, and dominates the gas flow in the inner Galaxy. To understand the structure and dynamics of the Galactic bar better is therefore of prime importance in the Gaia era.

Renewed interest in the Galactic bar and bulge has also been triggered recently by unprecedented new near-infrared (NIR) photometric and spectroscopic surveys of the inner Galaxy. In this contribution, we summarize recent work on the structural properties of the Galactic bar and bulge based on such survey data.

About two thirds of all large disk galaxies are barred (Eskridge et al., 2000), including our Milky Way. Historically, several perceptive papers already suggested in the 1970s that the non-circular motions seen in HI observations towards the inner Galaxy could naturally be interpreted in terms of elliptical gas streamlines (Shane, 1972; Peters, 1975). But it was not until the 1990s that the barred nature of the Milky Way bulge was considered established. This revised view of our Galaxy was

Ortwin Gerhard, Christopher Wegg
Max Planck Institute for extraterrestrial Physics, PO Box 1312, Giessenbachstr., 85741 Garching,
Germany, e-mail: gerhard@mpe.mpg.de, wegg@mpe.mpg.de

based on new data and ideas at that time: the NIR photometry by the COBE satellite (Weiland et al., 1994; Binney et al., 1997), enabling a global view of the bulge through the dust layer; new analysis of the inner Milky Way gas flows traced in longitude-velocity diagrams (Englmaier & Gerhard, 1999; Fux, 1999), in the context of triaxiality and bars in external galaxies; asymmetries in bulge star counts (Stanek et al., 1994; Lopez-Corredoira et al., 1997), and the newly measured optical depth for microlensing towards bulge fields (Paczynski et al., 1994; Bissantz et al., 1997). These data, as well as the kinematics of bulge stars available at the time (Zhao et al., 1994; Fux, 1997), could all be consistently explained in terms of a barred bulge model with its major axis in the first quadrant. 2MASS NIR star counts (López-Corredoira et al., 2005; Skrutskie et al., 2006), the cylindrical rotation in the bulge (Kunder et al., 2012; Ness et al., 2013; Shen et al., 2010), and other data have since confirmed and refined our understanding of the Galactic bar.

In external disk galaxies seen at low inclination, bars are easy to see but their vertical structure is not well-constrained. However, we now know from gas- and stellar-kinematic data that box or peanut-shaped (b/p) bulges in edge-on systems are related to bars (Merrifield & Kuijken, 1999; Chung & Bureau, 2004). Photometric data (Lütticke et al., 2000; Bureau et al., 2006) are consistent with predictions from N-body models that bars in galaxies generally consist of an inner three-dimensional (3D) part, the b/p bulge, and a more extended 2D part of the bar (Athanassoula, 2005). In these simulations, a bar first grows from an unstable disk and then becomes unstable to a buckling instability which leads to an inner boxy bulge (Combes et al., 1990; Raha et al., 1991; Athanassoula & Misiriotis, 2002). The bar can then grow further through angular momentum loss to the dark matter halo, and eventually go through a second buckling instability which leads to the formation of a strongly peanut-shaped bulge (Martinez-Valpuesta et al., 2006). Similar secular evolution has been observed also in cosmologically more realistic simulations of disk galaxies, such as dissipative collapse models (Samland & Gerhard, 2003; Ness et al., 2014), or hierarchical disk galaxy models in which strong feedback and the absence of significant mergers ensure a relatively quiescent star formation history (Martig et al., 2012; Guedes et al., 2013).

2 Bulge distances from K-band magnitudes of red clump giants

Red clump giants are immensely useful for star count studies of the Galaxy. They are He core burning stars with a narrow range of luminosities and colours, hence can be employed to map out the distant-dependent structure of the Galactic bulge. Using the α -enhanced BASTI isochrones for various metallicities at age 10 Gyr from Pietrinferni et al. (2004), a metallicity-averaged luminosity function of bulge red clump (RC) stars has Gaussian $\sigma(K) = 0.18$ mag, $\sigma(J - K) = 0.05$, and $M_{K,RC} = -1.72$ in the K_S -band (Wegg & Gerhard, 2013a). The K_S -band magnitude is slightly brighter than the value from solar-neighbourhood RC stars (Alves, 2000). In the colour-magnitude diagram, RC stars are spread because of varia-

tions in distance, reddening, age, and metallicity. The variations in absolute K_S -magnitude with age and metallicity are $\Delta_{\text{age}}M_{K,RC} \sim 0.03/\text{Gyr}$ at age 10 Gyr and $\Delta_Z M_{K,RC} \sim -0.28/\text{dex}$ (Salaris & Girardi, 2002). From the same study, for old stellar populations the number of RC stars per unit initial mass varies by $\sim 10\%$ for metallicities $\gtrsim 0.02$ solar. Therefore the distribution of RC stars is a good tracer of the stellar mass distribution in the bulge. Distances to individual RC giants in the upper bulge can be estimated with $\sigma_D \sim 10\%$. At low latitudes, residual dust extinction broadens the clump magnitude distribution, leading to $\sigma_D \sim 15\%$ at $|b| = 1$ deg (Gerhard & Martinez-Valpuesta, 2012).

3 The Galactic box/peanut bulge

The COBE data firmly established the boxy shape and the presence of longitudinal asymmetries in the Galactic bulge, which appears brighter and vertically more extended on the $l > 0$ side, but symmetric in latitude b (Weiland et al., 1994). These asymmetries are a signature of a triaxial bulge whose major axis is tilted in the Galactic plane relative to the line-of-sight (LOS) from the Sun to the Galactic centre (Blitz & Spergel, 1991). From these asymmetries, parametric and non-parametric bulge luminosity models were reconstructed (Dwek et al., 1995; Bissantz & Gerhard, 2002) and then used to study the influence of the Galactic bar on the gas dynamics and microlensing observations. However, uncertainties remained due to the lack of distance information in the COBE data and to the uncertainties in the extinction maps.

Red clump star counts in several fields across the bulge first illustrated the different distances to the near and far sides of the triaxial bulge (Stanek et al., 1994, 1997). With the 2MASS all sky data a first star count reconstruction of the bulge shape became possible, even if somewhat affected by the limit in the survey depth (López-Corredoira et al., 2005). More recent analysis of OGLE-III and 2MASS RC counts in upper bulge fields near the minor axis showed the presence of two density peaks along the LOS (Nataf et al., 2010; McWilliam & Zoccali, 2010). These results were interpreted as an X-shape in the bulge density distribution such as seen in N-body models of peanut bulges. Abundances and velocities derived from spectra of large numbers of bulge stars showed that only the more metal-rich stellar populations participate in this 'split red clump' (Ness et al., 2012).

The recent VVV survey is $\sim 3 - 4$ mag deeper than 2MASS and RC stars are visible all through the bulge even quite close to the Galactic plane. These data have brought a quantum leap for constraining the bulge density distribution. First results at $b = \pm 1$ deg showed clearly the in-plane tilt of the barred bulge, and also a structural change in the central $|l| < 4$ deg (Gonzalez et al., 2011), indicating a less elongated distribution of stars in this region (Gerhard & Martinez-Valpuesta, 2012). In our recent work (Wegg & Gerhard, 2013a), we used the VVV DR1 data (Saito et al., 2012) for some 300 sightlines across $|l| < 10$ deg and -10 deg $< b < 5$ deg, to measure the 3D density distribution of the Galactic bulge. For all these LOS, we con-

structed extinction- and completeness-corrected K_S -band magnitude distributions, and deconvolved these with the K-band luminosity function of RC giants and red giant branch bump (RGG) stars. The extinction model was determined from the RC stars themselves, with a method very similar to Gonzalez et al. (2011). Completeness effects were corrected based on artificial stars inserted in the VVV images. For the deconvolution we used a Lucy-Richardson scheme including a 'background component' of stars not in the RC+RGG. This is a good approximation because the magnitudes of these stars vary over a wide range. The deconvolved LOS density distributions clearly show the split red clump at latitudes $|b| \geq 4$ deg.

For constructing the entire 3D bulge density distribution, we then assumed that the bulge is eightfold triaxially symmetric. This assumption can be checked at the end: the rms deviations between the mirror-symmetric points in the final model are indeed small. Finding the best eightfold symmetric distribution determines the tilt angle of the bar-bulge to the LOS to be (27 ± 2) deg, where the dominant error is systematic, arising from the details of the deconvolution process. Our final density map covers the inner $(2.2 \times 1.4 \times 1.1)$ kpc of the bulge/bar. It is illustrated in Figures 1 and 2. The density is typically accurate to $\sim 10\%$ except at $y > 1$ kpc along the intermediate axis of the bar. In the projected density maps shown in Figs. 1, the region $|b| < 1$ deg was extrapolated from $b \geq 1$ deg with a simple sech^2 -model (Portail et al., in preparation), because at these low latitudes the extinction and completeness corrections are too large for a reliable density deconvolution.

Fig. 1 shows a highly elongated bar, with projected axis ratios $\approx (1 : 2.1)$ for isophotes reaching major axis radii ~ 2 kpc. Above about 400 pc above the Galactic plane, a prominent X-structure is visible which explains the earlier measurements of the split red clump. This X-structure is characteristic for a class of b/p bulges (Bureau et al., 2006). In fact, the b/p bulge of the Milky Way is very strong, about as strong as in the proto-typical b/p bulge in NGC 128 (Wegg & Gerhard, 2013b). Beyond about 1 kpc along the major axis, the iso-surface density contours in the edge-on projection bend down and outwards to the Galactic plane.

4 Does the Milky Way have a diskly pseudo-bulge?

Along the principal bar axes the density falls off approximately exponentially, as shown in Fig. 2. Exponential scale-lengths are $(0.70:0.44:0.18)$ kpc, corresponding to axis ratios $(10:6.3:2.6)$. The flattening of the major axis profile beyond ~ 1 kpc signifies the transition to the longer, planar bar.

Particularly noteworthy is the very short vertical scale height in the centre, perhaps indicative of a central disk-like, high-density pseudo-bulge structure as is seen in many early and late type b/p bulge galaxies (Bureau et al., 2006), including the edge-on Milky Way analogue NGC 4565 (Kormendy & Barentine, 2010).

Additional support for this interpretation comes from the change-of-slope at $|l| \simeq 4$ deg seen in the VVV RC star count maxima longitude profiles for $b = \pm 1$ deg (Gonzalez et al., 2011; Wegg & Gerhard, 2013a). The simplest interpretation of this

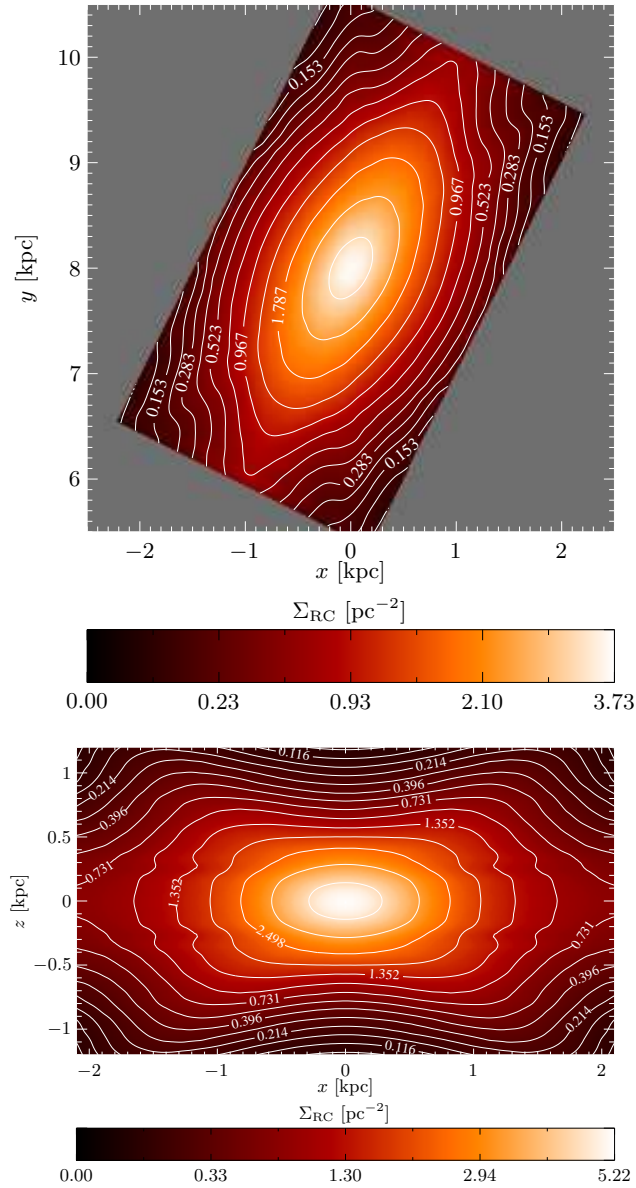


Fig. 1 (a), top: The Galactic bulge as viewed from the north Galactic pole. **(b), bottom:** The bulge 3D density projected along the intermediate axis. Numbers give the surface density of RC stars in pc^{-2} , contours are spaced by $1/3$ mag. The 3D density map extends to 1.15 kpc along the minor axis and to 1.4 kpc along the intermediate axis, and the projections are within these limits.

result is the presence of a rounder, more nearly axisymmetric central part of the bar, as illustrated by Gerhard & Martinez-Valpuesta (2012) with an N-body model with this property (see Figure 3). In fact, if the central parts of the Milky Way bar were completely axisymmetric, the inner slope of the longitude profile would be nearly zero. This model also predicted that the transition to a rounder inner parts was confined to a few degrees from the Galactic plane. This was later confirmed with VVV data by Gonzalez et al. (2012). However, more work is required particularly at low latitudes to confirm a diskly pseudo-bulge in the Milky Way.

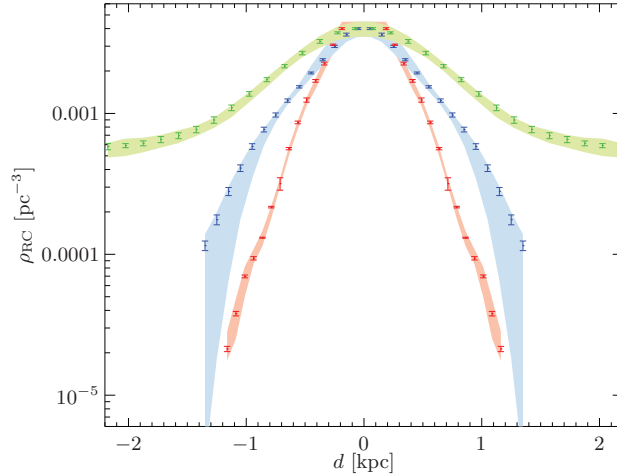
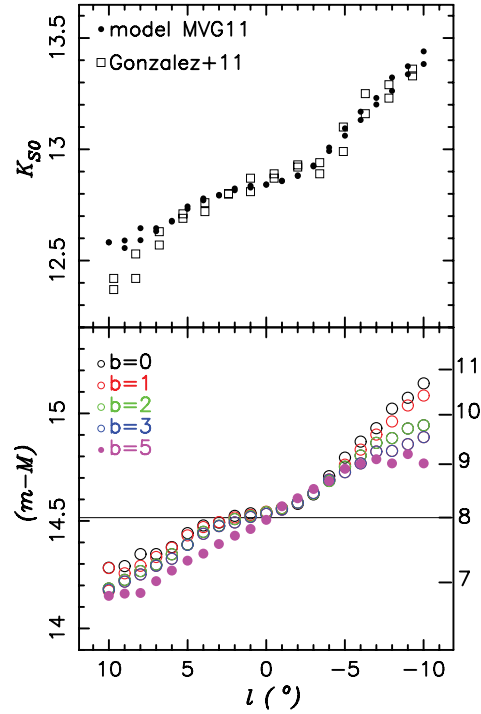


Fig. 2 Density of RC stars along the major axis (green), intermediate (blue), and minor axis (red) for the bulge. The major and intermediate axis profiles are offset from the Galactic plane by 187.5 pc. The error bars are the rms deviations between the eightfold symmetric points of the final bulge density distribution. The shaded regions show estimated systematic errors based on varying the details of the deconvolution procedure. From Wegg & Gerhard (2013a).

5 The long bar

Hammersley et al. (2000) first drew attention to an overdensity of stars in the Milky Way disk plane reaching outwards from the bulge region to $l \simeq 28$ deg. This structure was confirmed in several subsequent NIR star count investigations, e.g. with UKIDSS (Cabrera-Lavers et al., 2008). Due to its longitude extent and the narrow extent along the LOS it was termed the ‘long bar’. In Spitzer Glimpse mid-infrared star counts (Benjamin et al., 2005), which are even less affected by dust, a corresponding long bar was inferred from a similar overdensity of sources observed on the $l > 0$ side. The long bar has a vertical scale-length of less than 100 pc, so is

Fig. 3 Maxima of RC magnitude distributions in the strips $b = \pm 1$ deg across longitude. In the top panel for VVV K-band counts from Gonzalez et al. (2011, open squares) and for an N-body model from Martinez-Valpuesta & Gerhard (2011, dots). The model reproduces the data well because its central parts near the symmetry plane are more axisymmetric than the main bar. In the bottom panel for slices through the model with different latitude as seen from the Sun. The change of slope seen in the simulated RC magnitude distributions for $|b| < 2$ deg is absent at $|b| = 5$ deg. From Gerhard & Martinez-Valpuesta (2012).



clearly a disk feature. Curiously, the orientation of the long bar inferred by all these investigations was at ~ 45 deg with respect to the LOS to the Galactic centre.

Such a misalignment of the long bar with the b/p bulge is difficult to understand dynamically. Two independent, misaligned barred structures with sizes differing by only a factor of ~ 2 would be expected to align quickly, due to the mutual gravitational interaction. Note that secondary nuclear bars are generally ~ 8 times smaller than the primary bars in their host galaxies (Erwin, 2011). Thus Martinez-Valpuesta & Gerhard (2011); Romero-Gómez et al. (2011) both argued that the long bar would more likely be the 2D part of the Milky Way bar continuing outwards from the 3D barred bulge, such as generally seen in secularly evolved N-body models. Martinez-Valpuesta & Gerhard (2011) predicted star counts from an N-body model with a bar and inner boxy bulge formed in a buckling instability. They argued that approximate agreement with the star count data could be achieved if the ends of the planar part of the bar have developed leading ends through interaction with the adjacent spiral arm heads. They found that such a configuration was present in their model for $\sim 40\%$ of the time in an evolutionary sequence from leading to straight to trailing, and also that some barred galaxies have bars with leading ends.

However, the star count maxima signifying the long bar (Cabrera-Lavers et al., 2008) show some discontinuities near $l = 10$ deg and $l = 20$ deg, and the LOS distance dispersion of these RC stars shows a large scatter when plotted versus longi-

tude. Therefore, in order to understand the Milky Way's planar bar better, we are currently reanalyzing the combined 2MASS, UKIDSS, and VVV surveys of the inner Galaxy (Wegg et al., in preparation). All data were extinction corrected and brought to a common photometric system. Fig. 4 shows the total star counts across the Galactic bulge and inner disk in a magnitude interval common to all surveys. From this map it is apparent that the vertical scale-height of the star counts decreases continuously from the maximum in the X-region of the b/p bulge into the planar bar and disk. This is confirmed more quantitatively by measuring the vertical gradients of the RC stars on the $l > 0$ side. There is no indication for two separate components in these plots. Investigation into the LOS distribution of RC stars versus longitude in the combined data is on-going. This will give us a better understanding of the long bar and the transition region between the bar and the adjacent disk in the Milky Way.

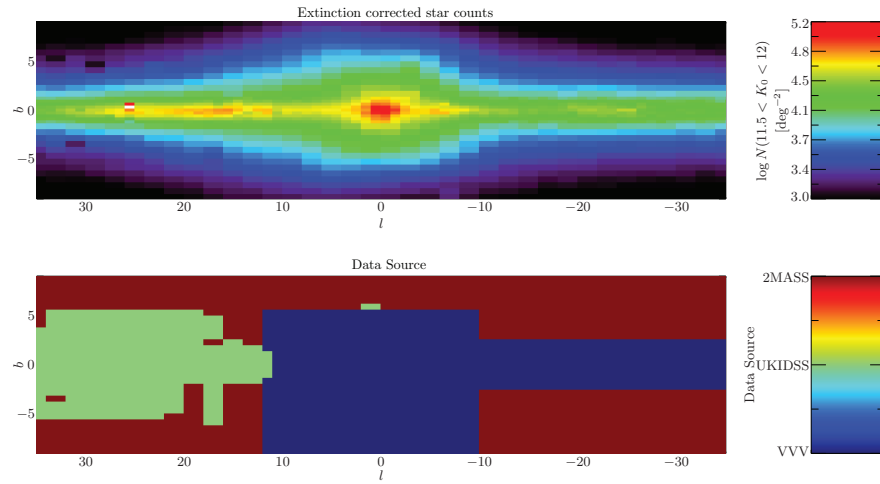


Fig. 4 The Galactic bulge and bar as seen from the Sun in K-band star counts combined from the cross-matched 2MASS, UKIDSS, and VVV surveys as shown in the lower panel. The magnitude range shown ($11.5 < M_K < 12$) is chosen such that the VVV data in the Galactic plane are not yet saturated and at the same time the 2MASS data are still complete in the region where they are used. This projection shows the continuous transition in the vertical scale-height from the inner 3D b/p bulge to the outer 2D bar.

References

- Alves D. R., 2000, *ApJ*, 539, 732
- Athanassoula E., 2005, *MNRAS*, 358, 1477
- Athanassoula E., Misiriotis A., 2002, *MNRAS*, 330, 35
- Benjamin R. A., Churchwell E., Babler B. L., Indebetouw R., et al. 2005, *ApJL*, 630, L149
- Binney J., Gerhard O., Spergel D., 1997, *MNRAS*, 288, 365
- Bissantz N., Englmaier P., Binney J., Gerhard O., 1997, *MNRAS*, 289, 651
- Bissantz N., Gerhard O., 2002, *MNRAS*, 330, 591
- Blitz L., Spergel D. N., 1991, *ApJ*, 379, 631
- Bureau M., Aronica G., Athanassoula E., Dettmar R.-J., Bosma A., Freeman K. C., 2006, *MNRAS*, 370, 753
- Cabrera-Lavers A., González-Fernández C., Garzón F., Hammersley P. L., López-Corredoira M., 2008, *A&A*, 491, 781
- Chung A., Bureau M., 2004, *AJ*, 127, 3192
- Combes F., Debbasch F., Friedli D., Pfenniger D., 1990, *A&A*, 233, 82
- Dwek E., Arendt R. G., Hauser M. G., Kelsall T., et al. 1995, *ApJ*, 445, 716
- Englmaier P., Gerhard O., 1999, *MNRAS*, 304, 512
- Erwin P., 2011, *Memorie della Societa Astronomica Italiana Supplementi*, 18, 145
- Eskridge P. B., Frogel J. A., Pogge R. W., Quillen A. C., Davies R. L., DePoy D. L., Houdashelt M. L., Kuchinski L. E., Ramírez S. V., Sellgren K., Terndrup D. M., Tiede G. P., 2000, *AJ*, 119, 536
- Fux R., 1997, *A&A*, 327, 983
- Fux R., 1999, *A&A*, 345, 787
- Gerhard O., Martinez-Valpuesta I., 2012, *ApJL*, 744, L8
- Gonzalez O. A., Rejkuba M., Minniti D., Zoccali M., Valenti E., Saito R. K., 2011, *A&A*, 534, L14
- Gonzalez O. A., Rejkuba M., Zoccali M., Valenti E., Minniti D., Schultheis M., Tobar R., Chen B., 2012, *A&A*, 543, A13
- Guedes J., Mayer L., Carollo M., Madau P., 2013, *ApJ*, 772, 36
- Hammersley P. L., Garzón F., Mahoney T. J., López-Corredoira M., Torres M. A. P., 2000, *MNRAS*, 317, L45
- Kormendy J., Barentine J. C., 2010, *ApJL*, 715, L176
- Kunder A., Koch A., Rich R. M., de Propris R., Howard C. D., Stubbs S. A., et al. 2012, *AJ*, 143, 57
- López-Corredoira M., Cabrera-Lavers A., Gerhard O. E., 2005, *A&A*, 439, 107
- Lopez-Corredoira M., Garzon F., Hammersley P., Mahoney T., Calbet X., 1997, *MNRAS*, 292, L15
- Lütticke R., Dettmar R.-J., Pohlen M., 2000, *A&A*, 362, 435
- Martig M., Bournaud F., Croton D. J., Dekel A., Teyssier R., 2012, *ApJ*, 756, 26
- Martinez-Valpuesta I., Gerhard O., 2011, *ApJL*, 734, L20+
- Martinez-Valpuesta I., Shlosman I., Heller C., 2006, *ApJ*, 637, 214
- McWilliam A., Zoccali M., 2010, *ApJ*, 724, 1491
- Merrifield M. R., Kuijken K., 1999, *A&A*, 345, L47

- Nataf D. M., Udalski A., Gould A., Fouqué P., Stanek K. Z., 2010, *ApJL*, 721, L28
- Ness M., Debattista V. P., Bensby T., Feltzing S., Roškar R., Cole D. R., Johnson J. A., Freeman K., 2014, *ApJL*, 787, L19
- Ness M., Freeman K., Athanassoula E., Wylie-de-Boer E., Bland-Hawthorn J., Asplund M., et al. 2013, *MNRAS*, 432, 2092
- Ness M., Freeman K., Athanassoula E., Wylie-De-Boer E., Bland-Hawthorn J., Lewis G. F., et al. 2012, *ApJ*, 756, 22
- Paczynski B., Stanek K. Z., Udalski A., Szymanski M., Kaluzny J., Kubiak M., Mateo M., Krzeminski W., 1994, *ApJL*, 435, L113
- Peters III W. L., 1975, *ApJ*, 195, 617
- Pietrinferni A., Cassisi S., Salaris M., Castelli F., 2004, *ApJ*, 612, 168
- Raha N., Sellwood J. A., James R. A., Kahn F. D., 1991, *Nature*, 352, 411
- Romero-Gómez M., Athanassoula E., Antoja T., Figueras F., 2011, *MNRAS*, 418, 1176
- Saito R. K., Hempel M., Minniti D., Lucas P. W., et al. 2012, *A&A*, 537, A107
- Salaris M., Girardi L., 2002, *MNRAS*, 337, 332
- Samland M., Gerhard O. E., 2003, *A&A*, 399, 961
- Shane W. W., 1972, *A&A*, 16, 118
- Shen J., Rich R. M., Kormendy J., Howard C. D., De Propris R., Kunder A., 2010, *ApJL*, 720, L72
- Skrutskie M. F., Cutri R. M., Stiening R., Weinberg M. D., et al. 2006, *AJ*, 131, 1163
- Stanek K. Z., Mateo M., Udalski A., Szymanski M., Kaluzny J., Kubiak M., 1994, *ApJL*, 429, L73
- Stanek K. Z., Udalski A., Szymanski M., Kaluzny J., Kubiak M., Mateo M., Krzeminski W., 1997, *ApJ*, 477, 163
- Wegg C., Gerhard O., 2013a, *MNRAS*, 435, 1874
- Wegg C., Gerhard O., 2013b, *The Messenger*, 154, 54
- Weiland J. L., Arendt R. G., Berriman G. B., Dwek E., Freudenreich H. T., Hauser M. G., et al., 1994, *ApJL*, 425, L81
- Zhao H., Spergel D. N., Rich R. M., 1994, *AJ*, 108, 2154